RESEARCH ARTICLE OPEN ACCESS

The Use of Optical Remote Sensing For Mapping Flooded Areas

Igor Ogashawara*, Marcelo Pedroso Curtarelli* and Celso M. Ferreira**
*(Remote Sensing Division, National Institute for Space Research, Brazil)
** (Department of Civil, Environmental and Infrastructure Engineering, George Mason University, USA)

ABSTRACT
Flood maps are a crucial tool to support emergency management, disaster recovery and risk reduction planning. Traditional flood mapping methods are time-consuming, labor intensive, and costly. Our goal in this paper is to introduce a novel technique to aggregate knowledge and information to map coastal flooded areas. We proposed a Difference of Normalized Difference Water Indices (DNDWI) derived from two LANDSAT-5/TM surface reflectance product acquired before and after the passage of Hurricane Ike, for Upper Texas in September of 2008. The reference flooded area was delineated interpolating the maximum surge in each location using a spline with barriers method with high tension and a 30 meter Digital Elevation Model (DEM). It was noticed that NDWI values decreased after the hurricane landfall on average from 0.226 to 0.122 for flooded area. However for the non-flooded areas it increased from 0.292 to 0.300. Results from the Monte Carlo simulation showed that mapping flooded areas with DNDWI got an accuracy of 85.68% while the non-flooded areas got an accuracy of 92.13%. Thus, DNDWI is promising tool for mapping flooded areas since it is a cheaper and simple technique which can be applied rapidly for several areas of the planet.

Keywords - Flood mapping, Hurricane, Monte Carlo Simulation, NDWI, Optical Remote Sensing

I. INTRODUCTION

Hurricanes are one of the most costly natural disasters in the United States [1] and recent storms such as Hurricane Sandy (2012), Ike (2008) and Katrina (2005) have caused major infrastructure damage and losses of lives along the East and Gulf Coasts [2]. Tropical cyclones are also a major cause of flooding and damage in several regions worldwide including recent events in the Bay of Bengal, Typhoon Phailin (2013), and historically deadly storms such as Tropical cyclone Thelma (1991), in the North Pacific Ocean, and Cyclone Zoe (2002), in the South Pacific Ocean, among others. Coastal flooding is one of the major hazards to accompany a tropical cyclone landfall [3] and can be aggravated by the combination of the storm tidal surge and rainfall-runoff from the heavy precipitations.

Traditionally, coastal flooding due to tropical cyclones has been estimated by measured water levels on buoys and coastal gages (e.g., [4-5]). Although these monitoring networks provide good historical data for coastal flooding, it lacks spatial information due to the limited number of stations over large areas. Recent developments of physics based numerical models using High Performance Computing (HPC) (e.g., [6]) in addition to an increasingly large volume of high resolution data (e.g., topo/bathymetry, land use, wind fields) has led to an unprecedented improvement in accuracy of tropical cyclones flood prediction and mapping. A combination of numerical modeling and measured data for model validation and calibration is currently the state of the art in predicting coastal flooding [7]. Recently the United States Geological Survey (USGS) launched the Inland Storm-Tide Monitoring Program [8] that provides unprecedented detail in coastal flooding monitoring during hurricane events on the United States coastal areas. Although recent advances in technology and methods, the forecasting and mapping of coastal flooding spatial extent is still a challenge especially in large areas without extensive instrumentation.

In this way, remote sensing data can provide useful information to mapping coastal flooding over large area. The main advantages in the use of remote sensing data are the synoptic view of large areas, spatial variability of data and repetitive acquisition. Moreover, the cost of data acquired by sensors onboard orbital platforms can be lower than the data acquired by conventional methods (discounting the cost of the satellites) [9]. Recently, remote sensing data have been applied to identify flood areas using the Environmental Satellite (ENVISAT) advanced synthetic aperture radar (ASAR) and Landsat Thematic Mapper (TM) optical imagery to document the flooded extent of Hurricane Ike (2008) by [10]. Subsequently, [11] presented a summary of the limitations and potentials of satellite imagery to monitor and map coastal flooding for Hurricanes Gustav and Ike (2008) demonstrating that the correspondence between ground data and ASAR-based flood mapping ranged from 86 to 96% for water levels higher than 0.8 m.

Although the good correspondence between ground data and RADAR-based flood mapping, such as demonstrated by [11], RADAR (Radio Detection and Ranging) sensors (e.g., ASAR, TerraSAR, RADARSAT) are not always imaging freely and generally their products have high costs. Moreover,

the data acquisition is sparse and over small areas. Therefore, it is necessary to develop new techniques based only on optical remote sensing data, which generally is available freely, have more options of spatial and temporal resolutions and has a historical time series with more than 10 years records (e.g., MODIS and TM sensors), which allows mapping the flooding extent of past events.

The objective of this study is to introduce a novel technique based on optical remote sensing techniques in order to aggregate knowledge and information to map coastal flood areas. We present a case study for the coastal flooding caused by Hurricane Ike on the Texas coast and develop our method using the Normalized Difference Water Index (NDWI) which was derived from two the medium resolution LANDSAT-5/TM surface reflectance product from the LANDSAT Climate Data Record (CDR).

II. STUDY AREA AND EVENT

The study area is the upper Texas coast, USA, which was directly impacted by Hurricane Ike in 2008 more specifically between the coordinates 30°46'23"N 95°41'48"W and 29°19'53"N 94°1'57"W (Fig. 1). According to [12], the frequency of hurricanes in this region is one about every six years and the annual probability of hurricanes occurrence is around 31%. However, more than 40 events were registered in the past century (1 at each three year), which indicates an increase in the frequency of events.

Hurricane Ike was a Category 2 hurricane when it made landfall on the Texas coast [2] causing severe damage to the State of Texas, Bahamas and Cuba as well. The storm winds reached 230 km h^{-1} with the lowest central pressure at 935 mbar leaving an estimated death toll of 103 people and around 40 billion dollars in damages.

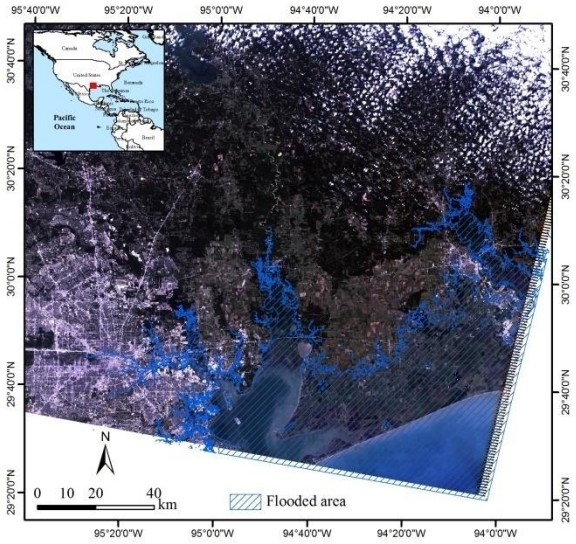

Figure 1. Study area in the Upper Texas, near Hilton and reference flooded area. LANDSAT-5/TM image acquired on 4 September true color composition.

III. DATASET

The dataset used in this study include in situ measurements and remote sensing images. The in situ data were collected by the USGS mobile storm surge network [8], which provide atmospheric pressure and water level data at each 6 minutes. The data were measured using a pressure transducer (HOBO Onset®) and stored in the USGS database [8]. Topography was obtained from a Digital Elevation Model (DEM) dataset extracted from the National Elevation Dataset (NED) [13] representing the entire region topography at a resolution of 1 arc-second.

The remote sensing data comprise images collected by the TM sensor, onboard LANDSAT-5 satellite. This images are provided with 7 spectral bands (from the visible to thermal spectral regions), quantized in 8 bits and with 30 meters spatial resolution, except the thermal band which has 120 m spatial resolution. The images are acquired at each 16 days. In this study we used the surface reflectance product from the LANDSAT CDR. This product is generated from specialized software called Landsat Ecosystem Disturbance Adaptive Processing System (LEDAPS) which provide images converted for reflectance values and corrected for the atmospheric effects. More information about this product is available at [14]

IV. METHODS

4.1. REFERENCE FLOODED AREA

The reference flooded area was determined based on the methodology proposed by [15] and consists of spatially interpolating the maximum flood height at each monitoring station and calculating the water depths based on the DEM. For this study we considered 59 recording stations along the study area. The maximum water heights were extracted from the recorded time series to represent the maximum flood level at each location. A spatial interpolation using a spline with higher tension (weight of 20 as suggested by [15] was used to develop the maximum water level coverage for the region. The water depths were calculated by subtracting the maximum flood surface from the DEM using the vertical NAVD88 Datum for the region. The resulting coverage was re-classified to remove the dry areas defining the estimated flood extent.

4.2. NORMALIZED DIFFERENCE WATER INDEX

As vegetation is one of the most affected targets by flood in coastal areas, changes in its water content could be used to identify the affected areas. The NDWI, which is also called the leaf area water-absent index, could be an alternative for optical remote sensing to map flooded areas. It is possible since this index (1) estimates the water content within vegetation [16]:

$$NDWI = \frac{\rho(0.86\mu m) - \rho(1.24\mu m)}{\rho(0.86\mu m) + \rho(1.24\mu m)}$$

where, $\rho(0.86\ \mu m)$ is the reflectance at 0.86 μm and $\rho(1.24\ \mu m)$ is the reflectance at 1.24 μm.

According to [16], it measures the liquid water molecules in vegetation that interact with solar radiation. The NDWI has been widely used because it is less sensitive to atmospheric scattering effects compared with the NDVI. However, similar to the NDVI, the NDWI did not completely remove the soil background reflectance effects. Using Landsat-5/TM bands, the NDWI was estimated as follows (2):

$$NDWI = \frac{\rho(TM_{B4}) - \rho(TM_{B5})}{\rho(TM_{B4}) + \rho(TM_{B5})}$$

where, $\rho(TM_{B4})$ is the reflectance at LANDSAT-5/TM band 4 and $\rho(TM_{B5})$ is the reflectance at LANDSAT-5/TM band 5. We used band 5 (1.65 μm) as an approximation of 1.24 μm [16]. This procedure was previously described in several studies [17-19].

4.3. METHOD DEVELOPMENT

The use of NDWI to classify flooded areas from a hurricane event consists in analyzing NDWI values from two different dates (before and after the hurricane). The difference among the NDWI values from the two dates is here called Difference of NDWI (DNDWI). Two thousand values of DNDWI were used to classify flooded and non-flooded areas according to the established limits for each of these two classes. These limits were computed from the univariate statistics of DNDWI values from each of the reference class. Average and standard deviations for each class was used to determine the lower and upper limit to categorize the DNDWI values. The DNDWI threshold for each class was chosen as plus/minus one standard deviation from the mean value plus a constant (see Table 1 in the results and discussion section).

4.4. VALIDATION

It was used to validate the NDNWI classification a Monte Carlo Method (MCM). The MCM, also known as statistical simulation, is defined as any method that uses sequences of random numbers to perform a simulation. This process was based on the outcome of many simulations using random numbers to obtain a probable solution. This technique provides an approximate, quick answer and a high level of accuracy; however, it is possible that accuracy is increased with additional simulations [20]. We collected 2000 stratified points of the DNDWI image, each class (flooded and non-flooded) got 1000 random values each. From these values an average from 20 of them were calculated 10,000 times. These 10,000 average values were used to evaluate the proposed classification using the thresholds analysis. The analysis were conducted by fitting all 10,000 values in the thresholds and them analyzing the number that got in the correct class.

V. RESULTS AND DISCUSSIONS

5.1. DNDWI CLASSIFICATION

For the DNDWI classification we collected 1000 points for each class based on the reference and calculate their univariate statistics and a histogram (Fig. 2). For the 1000 points from the flooded area, the average value was 0.107 while for the non-flooded are the average was -0.011.The median for the flooded area was 0.140 and the non-flooded got a median value of 0.003. It showed that the DNDWI is higher for flood areas and lower for non-flooded ones. It happened due to the fact that in both areas there were precipitation, however, as the NDWI measures the water content in the vegetation, at flooded areas the index was saturated while in non-flooded area it worked well.

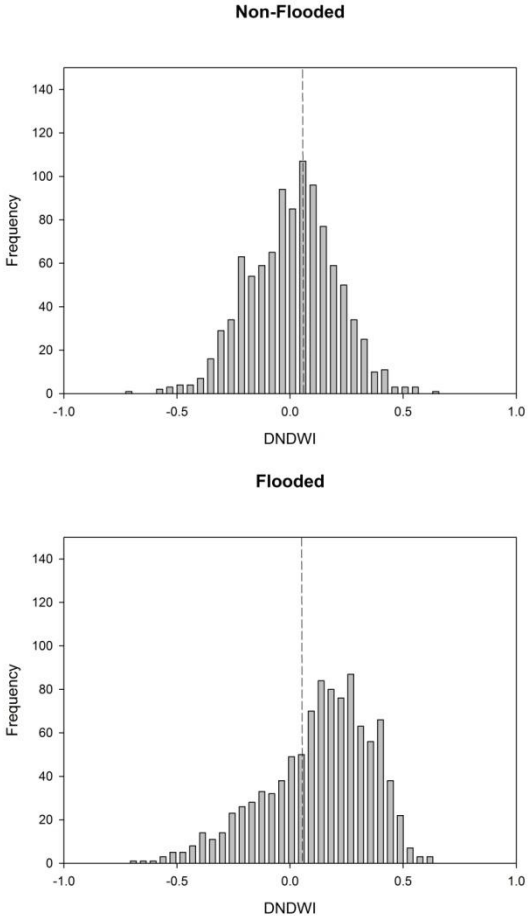

Figure 2. Histograms of DNDWI from the two classes according to the reference classification.

The values of DNDWI can be explained by the mean values of NDWI before and after the Hurricane Ike. The mean value of the NDWI before the hurricane was 0.292 for the non-flooded areas and 0.2264 for the flooded areas. They changed to 0.300 in the non-flooded areas and to 0.122 for flooded areas. It showed an increase of 2.74% in the NDWI values for the non-flooded area and a decrease of 45.82% of NDWI values for the flooded areas. Thus as the index values increases from the first to the second image in

the non-flooded areas, the DNDWI tends to decrease while the opposite is also true, in the flooded areas DNDWI values tend to increase due to the decrease of NDWI in the second image. Due to these characteristics the thresholds were calculated from the average plus/minus one standard deviation from the mean value plus a constant (Table 1).

Table 1. Thresholds for the DNDWI classification.

Classes	Threshold
Non-flooded	<0.05
Flooded	>0.05

5.2. VALIDATION USING MCM

To validate the choice of thresholds the 10,000 values from the simulated average of DNDWI values were analyzed. For flooded areas the values ranged from -0.099 to 0.285, while the values for non-flooded areas ranged from -0.193 to 0.143. The mean values of these two series were 0.106 and -0.010 for the flooded and non-flooded areas respectively. A histogram of all 10,000 DNDWI values and the threshold limit are shown on Fig. 3.

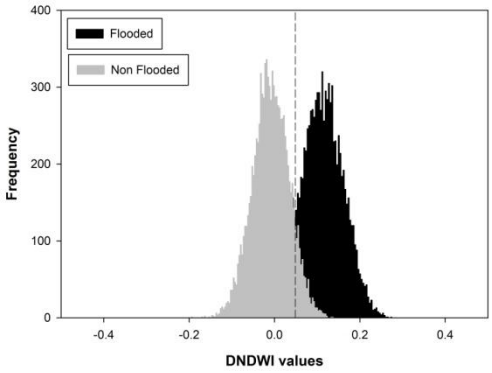

Figure 3. Histogram of DNDWI simulated average by MCM.

MCM results also showed that for flooded areas 8568 values were classified as flooded by the threshold analysis. For non-flooded the number of values in the range proposed in the threshold was 9213. It showed that DNDWI got an accuracy of 85.68% for mapping flooded areas, showing that it is a potential tool to help managers and policy makers to analyze the impacted areas.

We also calculate the results of the Wilcoxon signed rank test for the 10,000 values of DNDWI through the MCM. It showed that the null hypothesis was refuted with 5% significance (p-value < 0.001); thus, there was undoubtedly a difference in the DNDWI values from flooded and non-flooded areas.

VI. CONCLUSION

A methodology for mapping spatial variations of flood inundation caused by hurricanes events using optical remotely sensed image series was developed in this study. Since flood prevention, management and emergency response is an important issue for policy makers, flood detection using remote sensing can improve the number of monitored areas in remotely accessed places or in places without any monitoring program. As optical orbital sensors, like Landsat TM, ETM+ and OLI family, are collecting non-stop data from the entire planet, the use of an optical sensor could enhance the knowledge of flooding spatial mapping in areas with lack of data. Our results showed that the DNDWI and a threshold analysis method for distinguish flooded areas could be a potential tool to enhance the knowledge of tropical cyclones flooding mapping. It was observed, from a MCM technique, that 85.68% of 10000 mean values from an interaction of 20 to 1000 DNDWI values were accurately classified as flooded areas. For the non-flooded area an accuracy of 92.13% was found.

However, these results were based on only one event (Hurricane Ike) and should be extended to other study areas. We also observed that additional spectral behavior studies are needed to explain the relationship between water content and vegetation spectral response in flooded areas. Nevertheless, we proposed a methodology which could be an useful tool for countries without any flooding monitoring program and RADAR imagery cover, since the mapping of flooded areas is an important issue for the economy and the rebuilding of the affected region. Although the use of Synthetic Aperture Radar has been previously applied, the cost for buying the images is high as well as it is labor intensity. Using optical remote sensing is not only cheaper but also much easier to manage the data. Through the advance of orbital hyperspectral sensors like the Hyperspectral Imager for the Coastal Ocean (HICO), it will be possible to identify the key spectral ranges to identify the elevated degree of water content in vegetation. Thus the hyperspectral studies will enhance the use of optical remote sensing to map flooded areas.

VII. ACKNOWLEDGEMENTS

The first author is grateful to the Brazilian Federal Agency for Support and Evaluation of Graduate Education (CAPES) for the masters' scholarship. The second author wishes to thanks the National Counsel of Technological and Scientific Development (CNPQ) (grants 161233/2013-9) for the PhD scholarship.

REFERENCES

[1] N. Lott and T. Ross, *Tracking and Evaluating U.S. Billion Dollar Weather Disasters, 1980-2005*, National Climatic Data Center (NCDC), 2006. Available at: http://www1.ncdc.noaa.gov/pub/data/papers/200686ams1.2nlfree.pdf. Accessed on: 12 Oct 2013.

[2] National Oceanic and Atmospheric Administration (NOAA), *Tropical Cyclone Report: Hurricane Ike*, 2013a. Available at:

http://www.nhc.noaa.gov/2008atlan.shtml. Accessed on:10 Oct. 2013.

[3] D. Resio and J. Westerink, Modeling the physics of storm surges, *Physics Today*, *61(9)*, 2008, 33-38.

[4] National Oceanic and Atmospheric Administration (NOAA), *Tides and currents*, 2013b. Available at: http://tidesandcurrents.noaa.gov/. Accessed on: 15 Oct. 2013.

[5] United Nations Education, Scientific and Cultural Organization (UNESCO), *The Global Ocean Observing System (GOOS)*, 2013. Available at: http://www.ioc-goos.org/Accessed on: 11 Oct. 2013.

[6] J. Dietrich, M. Zijlema, J. Westerink, L. Holthuijsen, C. Dawson, R. Luettich, R. Jensen, J. Smith, G. Stelling and G. Stone, Modeling hurricane waves and storm surge using integrally-coupled, scalable computations, *Coastal Engineering*, *58(1)*, 2011, 45-65.

[7] C. Dawson, E.J. Kubatko, J.J. Westerink, C. Trahan, C. Mirabito, C. Michoski, N. Panda, Discontinuous Galerkin methods for modeling hurricane storm surge, *Advances in Water Resources*, *34(9)*, 2011, 1165-1176.

[8] United States Geological Survey (USGS), *The storm-tide monitoring program*, 2013a. Available at: http://water.usgs.gov/osw/programs/storm_surge1.html.Accessed on: 15 Oct. 2013.

[9] J.R. Jensen, *Remote sensing of the environment: An earth resource perspective* (Boca Raton, FL: Prentice Hall, 2006).

[10] E. Ramsey, D. Werle, Z. Lu, A. Rangoonwala and Y. Suzuoki, A case of timely satellite acquisition in support of coastal emergency and environmental response management, *Journal of Coastal Research*, *25(5)*, 2009, 1168-1172.

[11] E. Ramsey, D. Werle, Y. Suzuoki, A. Rangoonwala and Z. Lu, Limitations and potential of satellite imagery to monitor environmental response to coastal flooding, *Journal of Coastal Research*, *28(2)*, 2012, 457-476.

[12] D. Roth, *Texas Hurricane History*, National Weather Service, 2010. Available at: http://www.wpc.ncep.noaa.gov/research/txhur.pdf.Accessed on: 11 Oct. 2013.

[13] United States Geological Survey (USGS), *National Elevation Dataset*, 2013b. Available at: http://ned.usgs.gov/.Accessed on: 04 Aug. 2013.

[14] J.G. Masek, E.F. Vermote, N. Saleous, R. Wolfe, F.G. Hall, F. Huemmrich, F. Gao, J. Kutler, and T.K. Lim, A Landsat surface reflectance data set for North America, 1990-2000, *Geoscience and Remote Sensing Letters*, *3(1)*, 2006, 68-72.

[15] C. Berenbrok, R.R. Mason and S.F. Blanchard, Mapping Hurricane Rita inland storm tide, *Journal of Food Risk Management*, *2(1)*, 2009, 76-82

[16] B.C. Gao, NDWI - A Normalized Difference Water Index for remote sensing of vegetation liquid water from space, *Remote Sensing of Environment*, *58(3)*, 1996, 257–266.

[17] X.L. Chen, H.M. Zhao, P.X. Li and Z.Y. Yin, Remote sensing image-based analysis of the relationship between urban heat island and land use/cover changes, *Remote Sensing of Environment*, *104(2)*, 2006, 133–146.

[18] D.D. Bosch and M.H. Cosh, *SMEX03 Landsat Thematic Mapper NDVI and NDWI* (Boulder, CO: National Snow and Ice Data Center, 2008).

[19] T.J. Jackson and M.H. Cosh, *SMEX03 Landsat Thematic Mapper NDVI and NDWI* (Boulder, CO: National Snow and Ice Data Center, 2007).

[20] Y. Hong, K.-L. Hsu, H. Moradkhani and S. Sorooshian, Uncertainty quantification of satellite precipitation estimation and Monte Carlo assessment of the error propagation into hydrologic response, *Water Resource Research*, *42(8)*, 2006, 1-15.